DOE/NASA/12726-11
NASA TM-82686

NASA Redox Cell Stack Shunt Current, Pumping Power, and Cell Performance Tradeoffs

Norman Hagedorn, Mark A. Hoberecht,
and Lawrence H. Thaller
National Aeronautics and Space Administration
Lewis Research Center

February 1982

Prepared for
U.S. DEPARTMENT OF ENERGY
Conservation and Renewable Energy
Division of Energy Storage Systems

DOE/NASA/12726-11
NASA TM-82686

NASA-Redox Cell Stack Shunt Current, Pumping Power, and Cell Performance Tradeoffs

Norman Hagedorn, Mark A. Hoberecht,
and Lawrence H. Thaller
National Aeronautics and Space Administration
Lewis Research Center
Cleveland, Ohio 44135

February 1982

Work performed for
U.S. DEPARTMENT OF ENERGY
Conservation and Renewable Energy
Division of Energy Storage Systems
Washington, D.C. 20545
Under Interagency Agreement DE-AI01-80AL12726

SUMMARY

The NASA Redox energy storage system has been under active technology development since the mid 1970's. The hardware currently undergoing laboratory testing is either 310 cm^2 or 929 cm^2 (0.33 ft^2 or 1.0 ft^2) per cell in active area with up to 40 individual cells connected to make up a modular cell stack. This size of hardware allows rather accurate projections to be made of the shunt power/pump power trade-offs. The modeling studies that have been completed on the system concept are reviewed along with the more recent approach of mapping the performance of Redox cells over a wide range of flow rates and depths-of-discharge of the redox solutions. Methods are outlined for estimating the pumping and shunt current losses for any type of cell and stack combination. These methods are applicable to a variety of pumping options that are present with Redox systems. The results show that a fully developed Redox system will have acceptable parasitic losses when using a fixed flow rate adequate to meet the worst conditions of current density and depth of discharge. These losses can be reduced by about 65 percent if variable flow schedules are used. The exact value of the overall parasitics will depend on the specific system requirements of current density, voltage limits, charge, discharge time, etc.

INTRODUCTION

Within the past decade, several electrochemical systems have appeared that employ fluids that are pumped from a storage tank to a stack of cells where the actual electrochemical reactions take place. Zinc slurries were one of the first such fluids to be so used. Japanese (ref. 1) and French (ref. 2) investigators used them as the anode reactant in mechanically rechargeable zinc-air systems. These were followed by the zinc-halide systems, which used either chlorine (ref. 3) or bromine (ref. 4) as the cathode reactant. The adequate solubility of gaseous chlorine in zinc chloride solutions or the controlled solubility of bromine in bromide solutions provides the mechanisms by which these reactants in the elemental form are maintained at suitable concentration levels in their respective carrier solutions. These system concepts were closely followed by others using a fully soluble redox couple as the reactive specie for either the anode, the cathode (ref. 5), or both (ref. 6). Common to all these electrochemical system concepts was the desire to use a reactive species that was not burdened with the disadvantages of the more traditional electrode structure, where one electrochemical form of solid is transformed into another as the electrode undergoes charging and discharging reactions. In the more traditional electrode structure, a suitable mixture of solid material is usually affixed to an appropriate structure which lends mechanical support, physical dimensions, and electrical conductivity to the electrode. Aside from the tendency towards a variety of long-term decay mechanisms associated with this type of electrode configuration, the actual capacity is limited by the amount of reactive mixture that may be appropriately affixed to the mechanical support structure.

An inert electrode is defined as one that serves only to provide a path for electrons to and from the electrochemical reactions taking place at its surface. Reactions of the type Me^{+n}/Me^{+n+1} (redox), X_2/X^- (halogen) or Me (slurry)/$Me(OH)_n^{-m}$ can all take place at an "inert" electrode. The capacity of this type of electrode is limited only by the supply of the reactive material in the surrounding solution. At first glance these electrodes

would appear to be free from the life-limiting factors associated with the more traditional electrode structure, while permitting the separation of the storage-related and power producing-related portions of the overall battery system. Indeed, the electrochemical concepts associated with the use of flowing solutions have been a welcome addition to the general field of electrochemical energy storage. The infusion of thought and ideas provided by those with backgrounds in fluid flow, electrocatalysts, system control logic, etc., have resulted in the rapid technological development of a number of these new storage concepts.

As these different ideas have moved from the point of being single-cell laboratory curiosities to small multicell systems, the significance of the parasitic power required for the pumping of these liquids around the system has become more evident. The magnitude of this loss is magnified by two factors: First, small electrochemical storage systems, in which the power requirements might be from 2 to 10 kW, require rather small pumps (usually chemically resistant, magnetically coupled) that traditionally have very low efficiencies (5 to 20 percent); second, the minimization of shunt currents within stacks of cells that are connected in a bipolar manner requires the use of cell designs (narrow inlet and outlet ports), which result in high resistances to fluid flow.

In the development of the NASA Redox system, it has become increasingly evident that the single most important design feature is the sizing of the flow ports for the single cells of the system. This relates directly to the parasitic pumping losses of the system. In other system concepts as well, this design feature results from the rather complicated trade-off between shunt current, pumping power, and cell performance. For a given set of performance requirements (maximum current density, maximum depth-of-discharge, etc.), a minimum acceptable flow rate will result. Once this flow rate is known, the aforementioned trade-off will result in a sizing of the cell flow ports that will lead to an overall minimum in the sum of the losses due to shunt currents and pumping energy. It is intuitive that the cell designs that result in lower pumping losses would yield higher shunt current losses and vice versa.

In other systems as well, the parasitic losses associated with the pumping of reactant solutions may represent more of a barrier to the widespread use and adaptation of these new concepts than the actual technological problems related to their electrochemistry.

This paper will address itself primarly to the NASA Redox system. As will be pointed out, the electrode configuration, flow requirements, and flow schedule associated with this system are different from those for the other flow battery systems under development. Although only a limited generality exists, the overall methodology and discussion of the factors provide a basis for the evaluation of the pumping requirements of other concepts.

BACKGROUND

The NASA Redox system is an electrochemical storage device based on the use of two fully soluble redox couples and a highly selective ion exhange membrane. As such, it falls into the general class of flow batteries. Tanks are used to store the redox solutions, which are pumped through groups of cells that are called stacks. In these stacks the fluids flow in parallel through the respective cells. The cells themselves are connected in series elec-

trically through the use of conductive bipolar plates, which also separate the individual flow cells. Further detail and explanation of the electrochemical operation and the system-related features of this system are given elsewhere (ref. 7). Figure 1 illustrates the storage tanks, circulating pumps, and the types of cells that are contained within a typical stack. Figure 2 illustrates a typical stack of cells as they would be arranged in a full-function stack. The upper portion of this figure shows an expanded view of the individual parts that go into the basic building block of these systems - the single cell. Figure 3 depicts the hydraulic network of the parallel flow stack.

Using these three figures as a guide, the flow-related processes of the system may now be considered. The pumps draw fluid from their respective reactant storage tanks (fig. 1) and pump them into the inlet manifolds located along the bottom of the stack (fig. 3). The incoming liquid is distributed among the cells located within the stack. Thin slots, called inlet ports (fig. 2), conduct the fluid from the inlet manifold to the bottom part of the cell flow chamber where it can spread out from side to side before its slow vertical rise through a porous carbon electrode. The electrode is compressed between the bipolar plate on one side and the ion-exchange membrane on the other (fig. 2). A narrow free space above and below the electrode structure, but within the flow cavity, facilitates the spreading out at the bottom and the coming together at the top of the reactant solution. An exit port conducts the liquid into the exit manifold and from there back to the storage tank. The pressure drops that occur in this type of flow system are mainly in the plumbing lines to and from the stacks, in the narrow inlet and outlet ports located within the cells, and across the porous electrodes through which the solutions flow in the long direction (sheet flow).

The selection of an adequate flow rate for cells using fully soluble redox couples as reactants is complicated by the fact that there is a wide swing in the concentrations of the reactant and product species during the course of charge and discharge. For any fixed flow rate there is a corresponding variation in the number of reactant ions per unit time that enter each cell. As will be shown in more detail below, the flow rate is directly related to the maximum current that can be drawn from the cell at any given time. To maintain a constant rate of influx of reactant species into a cell, the flow rate must double each time the concentration is halved. It is clear that as a cell approaches either the fully charged or fully discharged condition, the minimum flow rate required to supply the stoichiometric quantity of reactant species to the cell cavity approaches infinity.

Whether a particular electrode structure performs well (even when adequate reactants are supplied to the cell) must be determined under actual operating conditions. The kinetic and mass transport characteristics of an electrode structure are difficult to assess without actual in-cell testing. The flow rate has a significant effect on the mass-transport characteristics of any particular electrode structure.

When the stack as a whole is considered, certain flow-related design features become very important. The ionic resistance of the fluid-filled reactant flow ports of the respective single cells has a significant effect on the magnitude of the shunt current losses that are experienced. The hydraulic resistance to the flow of these liquids across these same inlet and outlet ports is a major factor in determining the pump size (flow rate and head rise) for any given stack of cells.

The selection of flow-port dimensions for a given system is, of course, the result of an optimization procedure. The many factors that are involved in this selection require the systematic evaluation of (1) those physical effects that can be calculated directly, for example, cell-to-cell flow maldistributions, stack shunt losses, and pumping powers as a function of cell port dimensions, (2) the trade-offs between interacting parameters, for example, overall pressure drop and system maximum depth of discharge, and (3) the actual performance of a single cell at various flow conditions, for example, cell voltage as a function of flow rate, current density, and depth of discharge.

The following sections of this report will cover all these effects and interactions and delineate the approach taken which ultimately leads to the selection of the optimum flow port dimensions for various Redox cell design considerations. This final selection will result from minimizing the sum of the pump-power requirements and the shunt current losses for the particular Redox system under consideration.

Modeling Studies

Intrastack flow distribution. - From the hydraulic network shown in figure 3 it can be seen that the incoming flow to a manifold is divided between a number of inlet ports. With flow entrance at the bottom of the cells and exit at the top, the cells, as well as the inlet and outlet ports and the inlet and outlet manifolds, are completely filled at all times. Resistance to the flow of the liquids occurs both in the manifolds and across the cell (inlet port, cell cavity, outlet port). The distribution of the flow among the various cells can be estimated by knowing the ratio of the resistance to fluid flow across the cell to that down a segment of the manifold. Figure 4 is the schematic representation of this flow network problem, and figure 5 is the analytic solution of this problem for several ratios of flow resistance. For the case where the manifold resistance R_m is not small enough (or, the cell resistance R_c is too small), a significant symmetrical cell-to-cell flow rate variation will be present where a substantially higher-than-average flow occurs across the cells at both ends of the stack; whereas the cells at the center of the stack have a lower-than-average flow (solid curve, fig. 5). This effect becomes more significant as the average flow rate approaches the minimum allowable flow-rate condition. The center cell, all other things being equal, would be the first to suffer reactant starvation. As the ratio R_c/R_m increases, this is no longer a problem (dashed curves, fig. 5), and the distribution of flow rates will be affected more by variations in the individual cell resistances, which would be expected to possess a certain degree of randomness.

Shunt current modeling. - When common, ionically conductive fluid paths connect a group of cells that are electrically in series and when potential gradients exist, shunt currents will flow, unless some special technique is used to break the ionic circuits (ref. 8). The effect of these currents on the stack of cells in question is dependent on the exact system under consideration. In the case of fully soluble redox couples, the effects of shunt currents will manifest themselves as a reduced ampere-hour efficiency. Where plating/deplating electrodes are present, the added effect of shunt currents is the gradual redistribution of solid electroactive material in a systematic manner along the stack of cells, depending on the net shunt currents of the

individual cells. Further, the danger of metallic dendrite formation and propagation along the shunt paths is ever present. For the NASA Redox system, which uses two inlet and two exit manifolds, an early shunt-current model was developed (ref. 9; see fig. 6). This model assumed a break in the flow path somewhere outside the stack (e.g., the shunt paths connecting the stack to the tankage are disregarded); also, it was assumed, for simplicity, that there were no kinetic or mass-transport contributions to the mathematical description of the single-cell polarization characteristics. With these assumptions, the electric-circuit analog of a Redox stack was solved via a Kirchoff's Law analysis using a computer to generate and solve the $4n + 1$ loop equations, where n is the number of cells in the stack. Figures 6 and 7 show, respectively, a diagram of a four-cell stack of cells and the associated electrical analog network. Because of the nearly reversible behavior of these Redox electrodes, the assumption that Redox cell current-voltage characteristics can be approximated by the straight line relationship

$$E_{cell} = E_{open\ circuit} - IR$$

simplifies the solution of the network loop current equations significantly. The variables that are inserted into the program are directly related to the physical parameters of the cell and stack design; for example, the open-circuit voltage, the internal resistance of the cell, the ionic resistances of the inlet and outlet ports, the ionic resistance along the length of manifold from one cell inlet to the next, the number of cells in the stack, etc. The solution to this problem for a set of typical cell parameters is presented graphically in figure 8 for a 40-cell stack. The variation in the actual shunt currents from cell to cell along the stack is clearly seen, as is the slight effect this has on the individual cell voltages. The existence of higher shunt currents at the center of the stack results in two general effects that are important over and above the gross parasitic power loss, which is also calculated by the computer program. The first, which does not appear in this Redox system, is the gradual redistribution of any solid reactive material during the course of a number of charge/discharge cycles or during a long stand time at open circuit. The second, and one of particular concern for Redox stacks, occurs in the no-flow, open-circuit condition after the center cells have discharged completely, while the end cells still have some capacity (and thus cell voltage) remaining. These end cells can drive the center cells to rather low cell voltages or to actual reversal, wherein the possibility exists that any electrocatalyst that may be present could be anodically dissolved.

The shunt current model was used to generate a series of gross shunt loss values over a spectrum of cell design parameters and stack configurations. Table I is a simple listing of some of these values. Of particular significance is the very rapid increase of these expected shunt losses as the overall stack voltage is increased (more cells/stack or higher cell voltage/cell). Figure 9 is a plot of these results, showing that the shunt loss increases with an exponent between two and three as the number of cells per stack is increased. When high system voltages are desired, the suggested design is one where lower-voltage substacks are hydraulically placed in parallel and electrically placed in series. There is then the additional factor of stack-to-stack shunt currents, but these can be made small compared with the shunt losses resulting from the alternative, higher-voltage stacks. This comparison

favors the use of stacks of cells that are hydraulically placed in parallel and electrically in series because of the fact that the ionic resistances in the parallel feed lines to and from the stacks can be made rather high so that the sum of these losses when added to those of the low-voltage substacks is lower than the intrastack losses of a high-voltage stack.

Attempts to verify this model in operating hardware will be covered in the Experimental Studies section of this report as will be the trade-off resulting from lowering the shunt losses by decreasing the flow port cross sectional areas at the expense of higher pumping losses.

Minimum flow requirements. - As noted earlier, the range of flow requirements over the course of charge and discharge is considerable. This is caused by the changes in the concentrations of the reactant species as the ratios of Fe^{+2}/Fe^{+3} and Cr^{+3}/Cr^{+2} change during the course of a charge or a discharge. The minimum flow rate for a cell, which was referred to earlier as the stoichiometric flow rate, can be understood in terms of some basic chemical and electrochemical principles. A Faraday of electricity (Avogadro's number of electrons) is by definition 96 500 A•sec or 26.8 A•hr. A solution that contains 1 mole of ions per liter, by definition, contains Avogadro's number of ions per liter. If these ions undergo electrochemical reactions that involve but one electron per ion, then 1 liter of a 1 molar solution of this type of ion would produce 26.8 A•hr of electricity, if all of the ions were converted from one valence state to another. Considering flow rates, if a fully charged solution was directed into an electrochemical cell at the rate of 1 liter per hour, in principle, a continuous current of 26.8 A could be drawn from the cell. The existing solution would be completely depleted of reactant species. If the solution was 1/2 molar instead of 1 molar or had already been 50 percent converted from one ionic specie to the other, then 13.4 A would be the maximum continuous current that could be withdrawn from the cell. Doubling the flow rate would result in doubling the current. The stoichiometric flow rate is also a function of cell size if the current density is held constant since a doubling of the size would require twice the flow rate. For the case of a 929 cm^2 (1.0 ft^2) cell and solutions that are 1 molar in total Fe and Cr, the stoichiometric flow rates F_{SF} at two different current densities are shown in figure 10.

These plots are solutions of the equation written as

$$F_{SF} = \frac{\text{cell current (A)}}{\text{total concentration } \frac{(A \cdot sec)}{ml}} \times \frac{1}{\frac{1 - (\text{depth-of-discharge})}{100}}$$

for the case of a one electron reaction. As the term [1 - (depth-of-discharge)]/100 approaches zero, the stoichiometric flow rate increases very rapidly. During the charge portion of the cycle, curves similar to those in figure 10 that have very high flow rates at the high states of charge would result. The actual flow requirements will, of course, be greater than these calculable minima, due to mass transport considerations and cell-to-cell flow variations; but it has been found convenient to express the actual flow rate as a multiple of the stoichiometric flow rate. Table V presents the stoichiometric flow rate as a function of cell size, current density, and depth of discharge.

Experimental Studies

Shunt current studies. - The shunt current model (ref. 9), developed for the case of two circulating, ionically conductive electrolytes, had several assumptions built into it, such as reversible electrode kinetics and breaking of the electrolyte path outside the electrochemical stack. Less obvious assumptions relate to constructional aspects of the cell and stack hardware. The model does not allow for any conductive paths (ionic or electronic) other than the circulating electrolytes themselves. The ionically conductive membrane must not contact the electrolytes in the manifold or port areas since this would represent an unaccounted-for segment in the electrical shunt network. Likewise, the electronically conductive bipolar plate material must be isolated from the electrolytes in the manifolds. These considerations led to the use of dielectric washers (fig. 2) in the manifold areas of both the bipolar plates and the membranes. Although the membrane washer adequately protects the inner circumference of the manifold and the portion of the inlet and outlet ports closest to the manifold from these additional shorting paths, the inner portions of the narrow ports are still exposed to the membrane. The constructional features of most of the hardware in current use are thus not in complete compliance with those features assumed by the shunt current model. An extra dielectric gasket sheet between the membrane and the flow field would remove this difference. Short stack work is now underway that employs this extra sheet. The shunt current model output was compared with the data from stacks (5, 14, and 40 cell) of operating Redox hardware (table II). This comparison is very simply done, since the sum of all the various shunt currents can be measured directly as follows: When a stack of Redox cells is placed on charge at constant voltage, the charging current gradually tapers back as the system approaches full charge until there is an exact balance between the rate at which the solutions are charging and the rate at which the solutions are discharging via the internal shunt loops. When the charging of the fluids via the external charging current is precisely balanced by the discharging of the fluids via the various shunt current paths, a form of dynamic equilibrium exists. From then on, the state-of-charge and the charging current remain constant with time.

In table II the difference between the predicted value of 0.008 A and the measured value of 0.012 A is significant. It is still possible that, even using the dielectric washers and gaskets, there may be some minor electrolyte seepage at certain points. In the cell and system modeling and trade-off studies, the shunt current model is assumed to be correct. Later, as larger stacks of cells with completely insulated membranes are constructed and tested using the taper current technique, it will be decided whether some slight corrections should be made in the shunt current model. At this point only the 5- and 14-cell stacks have been constructed using the covered flow ports technique.

Cell and stack pumping requirements. - Reference 10 outlines the procedures used to determine single-cell pumping-power requirements as a function of flow rate over a range of inlet and outlet port sizes and for two cell cavity thicknesses. Measurements were carried out using water, and the data were then corrected for the actual redox solution viscosities. The reader is referred to reference 10 for further details on this work. The output of the study is shown in table III, where the ideal pumping power requirement is presented for the various cell and stack configurations examined. The experi-

mental data are shown in figure 11, where the pressure drop across the cell is presented as a function of the flow rate. It can be seen that, for the case of a rather restricted flow configuration (case 1: narrow ports, thin flow field), the major contribution to the pressure drop is in the flow ports. For the more open case (case 2) the pressure drop across the felt electrode predominates. Because the pumping power is equal to the product of the flow rate and the pressure drop, the resulting pumping power versus flow rate relationship should be an even steeper function of the flow rate than is the pressure drop, as indicated in the calculated results presented in table III. The results tabulated in this table, along with those presented in table I, form the basis for the trade-off that exists between pumping power and shunt current losses.

Cell performance evaluation procedures. - The aforementioned trade-off between shunt losses and pumping losses will, of course, be strongly affected by the reactant flow rates. To hold pump-power requirements within reason, high flow rates will call for flow ports having relatively large cross-sectional areas. This will, in turn, result in relatively high shunt-current losses. Therefore, it is desirable to operate at flow rates as low as possible.

To determine minimum necessary flow rates, cell performance measured as a function of flow rate was compared with the results of an idealized predictive model. In this way it was possible to quantify the minimum flow required to sustain acceptable performance in regards to the mass transport losses.

The two general types of flow configurations used in cells with inert, flow-through electrodes are depicted in figure 12. The type in which the flow of the fluid is perpendicular to the plane of the electrode is traditionally referred to as "flow through". The type in which the flow of fluid is parallel to the plane of the electrode is traditionally referred to as either "flow-by" or "sheet flow".

For the Redox cells concentrated solutions are used; thus, the flow rates required to meet the stoichiometry requirements are very low. (A flow rate of 125 cm^3/min ideally will supply a 929 cm^2 (1 ft^2) cell operating at 100 A when the fluids are in the half-charged condition.) For this reason the sheet-flow configuration represents the more logical choice, because it results in a higher effective velocity within the electrode. For typical cell geometries the effective velocity (flow rate/flow area), in the case of sheet flow, is about two orders of magnitude greater (table IV) than for the flow-through case. High superficial velocities produce excellent mass transport. Pump power, shunt loss, and performance considerations call for minimum volumetric flow rates and maximum intracell flow velocities, both of which result from use of sheet flow electrodes. Less obvious advantages of the sheet-flow configuration are greatly reduced constructional complexity and lower internal cell resistance, since the porous conductive electrode is compressed between the bipolar plate on one side and the ionically conductive membrane on the other.

The evaluation procedures used in Redox cell and electrode performance studies are described in detail elsewhere (ref. 11) and will be presented here only in summary form. The model used is essentially a lumped-parameter approach which predicts the cell performance over the complete range of flow rates, depths-of-discharge, and current densities. Figure 13 depicts a typical comparison of measured and predicted cell performance. This figure is generated using Ohm's Law to estimate the Ohmic losses (IR contributions) and

the Nernst equation to estimate the effects of concentration changes that take place between the inlet and outlet of the cell. When actual cell data are added to this figure, it is referred to as a flow map of the cell.

The horizontal lines result from the IR contributions at the respective currents. The dashed lines include the change in voltage of the cell due to the change in redox ratios as the two solutions flow through their respective electrodes. At very high flow rates or very low currents, a small change in concentration takes place; while at low flow rates or high currents, a significant change in concentration takes place. The distance between the IR correction line and the Nernstian correction line is referred to as "droop". It is recognized that the use of a lumped parameter model for the cell disregards the distribution of current density within the cell, which could be described using the Butler-Volmar equation. But for the sake of the main intent of this evaluation method it was felt that a further improvement on the simple Nernst correction was not needed.

This figure was constructed for the case of iron and chromium solutions, each 1 molar in its respective reactant cation ($C_{Cr+2} + C_{Cr+3}$) = 1 = ($C_{Fe+2} + C_{Fe+3}$) and electrochemically matched in terms of state-of-charge ($C_{Cr+2} = C_{Fe+3}$). The open-circuit voltage of these solutions at 50 percent depth of discharge ($C_{Cr+3}/C_{Cr+2} = 1 = C_{Fe+2}/C_{Fe+3}$) is taken as 1.05 V, by experience.

The condition under which the concentration of the exiting solution drops to zero represents a boundary condition. This minimum flow rate is, as noted, the stoichiometric flow rate. It is determined, for any combination of cell current and inlet concentration, from a mass balance around the cell with the outlet concentration set equal to zero:

$$(C_{inlet} - C_{outlet}) = \frac{I}{F}$$

or

$$F_{SF} = \frac{I}{(C_{inlet} - 0)}$$

where I is the cell current (A), F is the flow rate (cm^3/min), and C is the concentration of active species ($amp\text{-}min/cm^3$). The average cell solution concentrations ($C_{inlet} + C_{outlet}$)/2 are used to calculate the Nerstian droop corrections. The lines representing constant multiples of the stoichiometric flow rate are derived by connecting the various flow rate and Nernstian droops, which result in the same multiple of the stoichiometric flow. The closeness with which the actual data follow the Nernstian correction lines is a measure of the mass transport characteristics of the cell/electrode combination. For the case illustrated the cell/electrode combination performed quite well down to flow rates about 1.5 F_{SF}.

Another evaluation procedure, again using only IR and Nernstian type corrections is illustrated in figure 14. This figure plots the actual performance versus the expected performance over a range of depth of discharge (DOD) while at a variable flow rate (a constant multiple of the stoichiometric flow rate). Here again, the closeness of fit is the measure of mass transport characteristics.

In the case of a constant, fixed flow rate, the "data" curve in figure 14 would show a slightly higher cell output. However, there would be a penalty paid for the greater pumping requirements. The constant flow rate would result in a smaller Nernstian droop at the shallower DOD, since the flow rate would be a much larger multiple of the stoichiometric flow.

Once adequate cell performance is verified in terms of flow rate over the range of DOD of interest, the shunt-loss - pumping-loss trade-off, as outlined in the preceding section, can be completed.

DISCUSSION AND RESULTS

Overall Considerations

The discussion thus far has focused on those aspects of a Redox system design that can be established through simple experimental measurements, modeling, and trade-off analyses - all hardware-oriented aspects, which form only a part of the overall design of a complete system. A complete design involves many trade-offs, ultimately governed by economics, not technology. It is through iterative, economic modeling that system characteristics, such as current density, DOD range, maximum DOD, flow rate, stack size, etc., are optimized. The analysis, of necessity, includes both capital and operating costs. To be complete, the goal of the iterative process must be to minimize the cost of delivered energy.

The characteristics that can be established by the measurements and analyses discussed in earlier sections are (1) the optimum stoichiometric flow multiple, determined from the flow map of performance versus flow rate at constant DOD and current density, (2) the ideal pumping power, determined from the relationship between flow rate and cell pressure drop, measured for a range of specific cell sizes and flow port geometries, and (3) the shunt losses calculated for ranges of cell and stack sizes and flow port geometries.

The interplay of economic and technical constraints in a system design can be observed by considering the question of how to divide into stacks the number of single cells required to meet a given system voltage. Figure 9 shows that placing all the cells in a single stack would cause an extreme intrastack shunt loss, which is an inefficiency that results in larger storage tanks, more reactants, and increased operating costs. Modeling shows that, from an efficiency standpoint, it is better to have multiple stacks, connected in series electrically and in parallel hydraulically, even though such an arrangement results in interstack shunt losses (which can be calculated using the same model as for a stack of single cells). In the extreme, the logic based on efficiency alone would call for all stacks in the system to be single cells, that is, for all cells to be separated, one from another, by ion-conducting (fluid) flow paths of high resistance. However, economic considerations, among others, would argue against such a complete dispersion of the cells and would indicate instead some optimum stack size.

A caution should be injected here, concerning excessive "fine-tuning" of the optimization process. For example, suppose that a single-cell flow map had shown adequate performance at 1.0 F_{SF}, and that a maximum DOD of 80 percent had been chosen. A system designed to these criteria would never reach the 80 percent DOD level without some cells being driven to low (or negative) voltages, because of insufficient flow. This would result either from the standard flow maldistribution shown in figure 5 or from tolerances allowed in

fabrication and assembly. Therefore, in this example a multiplier greater than one would be applied to the stoichiometric flow rate.

Measurements and analyses can be used to determine the single-cell flow port dimensions that will minimize the shunt power/pump power trade-off for a stack of Redox cells. The next section discusses that process for two concepts of operation: constant volumetric flow rate (varying multiple of the stoichiometric flow rate) and constant multiple of the stoichiometric flow rate (variable volumetric flow rate). A single stack of cells will be considered.

Constant Volumetric Flow Rate

For this case, the constant volumetric flow rate must be chosen to meet the worst possible conditions, that is, maximum current density and maximum DOD. (Generally, these would be assigned assumed values that would be adjusted through iteration.) The assumed current density and the desired total current would define the cell area. For these values of current and DOD, a flow map such as that in figure 13 would have to be obtained in order to define an adequate multiple of the stoichiometric flow rate for the worst-case conditions.

Knowing the required stack voltage and the worst-case single-cell voltage (from the flow map), the number of cells in the stack can be determined. This, plus the flow rate per cell, enables the use of data such as those in table III, to obtain the ideal pump-power requirements for a range of flow-port geometries (represented in table III in terms of manifold-to-manifold resistance"). Similarly, calculated data (e.g., see table I) can be generated and used for the shunt-power loss, also as a function of flow-port geometries. Figure 15 represents a typical summation of pump and shunt power, as a function of flow-port geometry (manifold-to-manifold resistance) for several stack sizes. The ranges of parameter values involved with this particular figure result in very flat minima for the curves. This will not always be the case.

An example of the determination of the minimum sum of the pump and shunt current losses for a particular set of assumptions will now be illustrated (see table VI for summary of assumptions and calculations). It will be assumed that a 40-cell stack of 929-cm^2 (1-ft^2) cells is to be designed for operation with 1 molar redox solutions at 53.8 mA/cm^2 (50 A/ft^2) and a maximum DOD of 90 percent. The question is, what should be the dimensions of the 20-cm-long inlet and outlet ports to minimize the sum of the shunt-power and pump-power losses. The gross output of this 40-cell stack is estimated from the performance of the current best cells to be 1800 W, averaged over the full discharge cycle (50 A/ft^2 at 0.9 V/cell and 50 percent DOD). The losses are calculated as outlined in the previous sections. If it is assumed that the pump power required to move the fluids through the entire system is double the requirement for the stack alone and that the parasitic losses during the charge portion of the cycle are equal to those during the discharge portion of the cycle, that is, that the lengths of the charge and discharge portions of the cycle are equal, then the calculated parasitic energy loss over a complete charge/discharge cycle is 9 percent.

Constant Multiple of Instantaneous Stoichiometric Flow Rate

In the preceding section the flow rate was selected, based on the worst-case situation and then held fixed over all conditions of current density and DOD. If the option were available to control the flow rate in an efficient manner, a considerable reduction in the system parasitics would be possible. The experimentation carried out to verify this possibility (ref. 11) entailed the use of a throttling valve to adjust the flow rate. This, of course, had no effect on the pumping energy. Perhaps a variable-stroke positive displacement pump, or a variable-frequency motor/pump combination, would permit efficient pump turn down. Figure 16 typically can be generated for a cell by assuming a certain amper-hour capacity once the relationships between cell voltage - flow rate (performance maps at various depths-of-discharge) and pumping power - flow rate are known. The flow rate assumed here was 2.0 x SF. In table VII a case similar to this example and three other cases are compared. The first is the case where the selected flow rate is 1.5 x SF. The lower flow rate would result in a lower output (calculated to be 70.3 W•hr versus 71.1 W•hr for 2.0 x SF) over an 80 A•hr discharge (from 10 to 90 percent DOD of a 100 A•hr solution capacity), for a typical single-cell configuration. The calculated time-integral beneath the pumping-power curve can be calculated to be 0.09 W•hr versus 0.17 W•hr for the 2.0 x SF case. These values can be very closely estimated once a wide variety of flow-rate - port-geometry tests have been carried out (ref. 10).

In both these cases, a 60 percent pumping efficiency has been assumed. For the two cases where the constant flow rate was assumed to be 1.5 x SF and 2.0 x SF (evaluated at 90 percent DOD), it can be seen that higher cell outputs result at the expense of the higher pumping requirements (0.85 and 1.60 W•hr, respectively). As before, several corrections have been added to the percentage pumping loss values to make them reflect more closely the actual situation. Each number was doubled to reflect the fact that, during the charge portion of the cycle, pumping must also be provided. (This assumes the charge time equals the discharge time.) The numbers were doubled again to account for pressure drops outside the stack, assumed here to be equal to that within the stack.

All other things being equal, a cell for use in a system in which variable flow is possible should have more restrictive flow ports than a cell for a system with constant (high) flow, to take advantage of the possibility of also lowering the shunt losses. A minimum sum of pump and shunt-power losses can now be determined for the variable flow-rate case in the same general way as for the constant flow-rate case (table VI), with one exception: the pump-shunt trade-off will be performed at the 80 percent DOD level instead of the 90 percent level. This 80 percent level has been found to be the value at which the total integral under the pumping power versus DOD curve has its midpoint in terms of watt hours. Therefore, a time-average pump power can be equated to the pump power required at 80 percent DOD. Repeating, then, the example presented for the fixed-flow rate case, but making 80 percent DOD the design point, results in a minimum combined loss rate for pumps and shunt currents of about 34 W or about 6 percent on a overall cycle basis, versus 9 percent for the constant flow case. This is to be compared with a 59-W loss rate for the constant flow-rate case. As expected, the minimum occurs at a much more restrictive flow port geometry (0.43 by 0.08 cm). This decrease occurs because of the lower overall flow requirements (pumping energy) of the vari-

able flow case. This permits the squeezing down of the inlet and outlet ports to reduce the shunt loss and still have a much lower sum of the pumping and shunt losses. Table VI compares these two examples in a side-by-side manner.

CONCLUDING REMARKS

The design of a Redox system calls for the resolution of a great many trade-offs, which must be solved by iterative procedures. Sometimes the trade-off can be decided on technical terms, but more often the criteria are economic, the goal being to minimize cost.

There is one trade-off in the design of a Redox system that can be handled in purely technical terms: that between the shunt current losses of a Redox stack and the power required to pump reactants through the stack. The trade-off obviously has economic ramifications, but it can be evaluated simply in terms of maximizing efficiency. The trade-off is necessary because shunt currents are decreased by restricting the reactant flow ports of the single cells; the pumping requirements are decreased by making the flow ports larger.

This trade-off evaluation, because it involves pump power, is tied directly to the reactant flow rates. These, in turn, are dictated by the maximum DOD chosen as a design point (which is, itself, probably being varied as part of a larger optimization process).

There were considered here two separate system concepts regarding flow rates. The first calls for an unvarying flow throughout a complete charge/discharge cycle. This flow must be sufficient to sustain system performance even under the worst conditions - maximum current density and maximum DOD - and is thus quite high. The trade-off will, therefore, call for open flow ports and, even at the optimum port design, high pump and shunt losses. High pump losses result because of the high flow rate, and high shunt power losses result because of the low ionic resistance of the fluid in the ports. The second system concept requires the flow rate to be varied continuously (or in small, discrete steps) in such a way that it is always some fixed multiple of the stoichiometric flow rate. For this case the DOD selected as the design point for the pump-shunt loss trade-off is 80 percent. As a first approximation, at least, it can be assumed that minimizing the sum of pump power and shunt power losses at this design point will result in a minimum total energy loss from these two contributors over a complete cycle: the combined rate of energy loss will be less than that at the 80 percent design point from 10 to 80 percent DOD (when flow rates are low) and greater from 80 to 90 percent DOD.

The first step in the trade-off analysis for either system concept is to determine an acceptable stoichiometric flow rate multiplier. This is done experimentally by measuring cell performance (voltage) as a function of reactant flow rate (for fixed current density and DOD) using a single cell of the size and configuration planned for the completed system. Ideally, the current and DOD maintained during this test would be the same as the system design point. However, for a particular cell, the acceptable flow rate multiplier seems to be quite insensitive to these two parameters, and thus may be determined from data involving other than the design point values. The flow rate multiplier obtained in this way, plus the design point DOD and current density, permit the calculation of the required design-point fluid flow rates. Next, data must be available or obtainable, for the cell size under consideration, giving the pressure drop across the cell at the design-point flow rate for a range of flow port geometries (or, flow port resistances).

To provide simple reference to these flow-port geometries, each is described by a "resistance" value, calculated from the port dimensions and the resistance of the ionic fluid filling it.

Finally, a mathematical model for shunt current losses is solved to give the shunt power for the given stack over the same range of port resistances as above. Adding the pump power and shunt power at various values of port resistance leads to the resistance, and port geometry, that gives a minimum sum.

If it turns out that the optimum ports are quite open, it will be necessary to consider whether the distribution of flow among the various cells of the stack may cause a problem. If the hydraulic resistance to flow through a cell is not much larger than the resistance to flow in the segment of manifold connecting adjacent cells, it is possible for the cells toward the center of the stack to be virtually starved, while those toward the ends carry a disproportionate share of the flow.

If it is possible to vary pump flow efficiently and inexpensively, the pump power-shunt current trade-off reveals that the system concept of varying the flow to maintain a constant multiple of the stoichiometric flow rate is, by far, the more efficient approach. A trade-off study, performed for each of the two possible flow management concepts, using the same assumptions in each case, showed that the combined parasitic power (pump and shunt) for the variable flow rate concept was about one-third less than that for the constant flow rate concept.

REFERENCES

1. Boba, H.: SAE Trans. Paper No. 710237, 1971.

2. Appleby, A.J.; Jacquelin, J.: and Pompon, J.P.: Electrochemical Society Extended Abstract 316, 1977.

3. Symons, P.C.: Proc. Intern. Conf. on Electrolytes for Power Sources, 1973.

4. Putt, R.A.: Proc. 14th Intersociety Energy Conversion Engineering Conf., 1979.

5. Zito, R.: U.S. Patent 3,719,526, 1973.

6 Thaller, L.H.: Proc. Ninth Intersociety Energy Conversion Engineering Conf., 1974.

7. Thaller, L.H.: NASA TM-79143, 1979.

8. Grimes, P., et al.: Electrochemical Society Extended Abstract 121, 1980.

9. Prokopius, P.R.: NASA TM X-3359, 1976.

10. Hoberecht, M.A.: NASA TM-82598, 1981.

11. Hoberecht, M.A.; Thaller, L.H.: NASA TM-82707, 1981.

TABLE I. - SHUNT LOSSES PER STACK AS PREDICTED BY NASA MODEL

Manifold resistance (cell to cell), Ω	Cell resistance (manifold to manifold), Ω	Nominal cell voltage, V					
		1.0			2.0		
		Number of cells per stack					
		20	40	80	20	40	80
		Shunt loss, W					
1.0	1 000	4.9	31	140	20	125	560
	2 000	2.5	18	99	10	72	396
	3 000	1.7	12	77	6.9	51	307
	6 000	.87	6.7	46	3.5	27	183
	12 000	.44	3.5	25	1.8	14	101
2.0	1 000	4.5	25	93	18.7	102	372
	2 000	2.5	16	72	9	64	290
	3 000	1.7	12	60	6.7	46	239
	6 000	.87	6.4	40	3.5	26	157
	12 000	.44	3.4	23	1.8	13	93

TABLE II. - PREDICTED AND MEASURED SHUNT CURRENTS IN 310-cm^2 REDOX HARDWARE

Number of cells per stack	Stack	Taper current, A
5	Predicted by model	0.008
	Measured, flow ports exposed to membranes	.030
	Measured, flow ports insulated from membranes by gaskets	.012
14	Predicted by model	0.056
	Measured, flow ports insulated from membranes by gaskets	.080
40	Predicted by model	0.390
	Measured, flow ports exposed to membranes	.865

TABLE III. - PUMPING POWER PER STACK AS CALCULATED FROM FLOW STUDIES

Cavity thickness, cm	Flow port dimensions, cm	Approximate resistance (manifold to manifold), Ω	Flow rate per cell to each electrode, cm^3/min								
			150			300			450		
			Number of cells per stack								
			20	40	80	20	40	80	20	40	80
			Ideal pumping power[a], W								
0.125	0.2 by 0.075	7600	5.2	10	21	----	----	--	----	--	--
	.4 by 0.075	3800	3.0	6.0	12	14	27	55	----	--	--
	.7 by 0.075	2500	2.5	4.9	9.8	10	21	41	24	48	96
0.250	0.2 by 0.200	2900	1.8	3.6	7.3	8.5	17	34	22	45	90
	.4 by 0.200	1400	1.3	2.7	5.3	5.4	11	22	12	25	49
	.7 by 0.200	1000	.96	1.9	3.8	3.8	7.7	15	9.0	18	36

[a]Approximate cell to cell resistance, 1.25 Ω; solution viscosity, 1.55 cS.

TABLE IV. - SUPERFICIAL FLOW VELOCITIES

FOR 929 cm^2 CELLS

[Electrode porosity, 80 percent]

Flow rate, cm^3/min	Sheet flow		Flow through	
	Electrode thickness, cm			
	0.125	0.250	0.125	0.250
	Flow velocity, cm/min			
50	16.4	8.2	0.0673	0.0673
100	32.8	16.4	.13450	.1345
[a]200	65.6	32.8	.2690	.2690
400	131.2	65.6	.5380	.5380
600	196.8	98.4	.8070	.8070

[a]This flow rate represents 3.46 times the stoichimetric flow rate (3.46 F_{SF}) for a 1-molar solution at 50 percent DOD and at a current density of 50 mA/cm^2.

TABLE V. - REPRESENTATIVE STOICHIMETRIC FLOW RATES

[1-molar solutions]

Depth of discharge	Cell size, cm^2 (ft^2)								
	310 (0.33)			929 (1.0)			4645 (5.0)		
	Current density, mA/cm^2 (A/ft^2)								
	53.8 (50)	107.6 (100)	215.2 (200)	53.8 (50)	107.6 (100)	215.2 (200)	53.8 (50)	107.6 (100)	215.2 (200)
	Flow rate, cm^2/min								
10	12	23	46	35	69	138	184	366	732
25	14	27	54	42	83	166	208	416	832
50	21	42	84	63	125	250	312	624	1248
75	42	84	168	125	250	500	625	1248	2496
90	104	208	416	312	624	1248	1560	3120	6240

TABLE VI. – COMPARISON OF RESULTS OF STACK OPTIMIZATION

Parameter	Source	Fixed flow rate	Variable flow rate
Depth of discharge (max.), percent	Assumed	90	90
Cell size, cm^2 (ft^2)	Assumed	929 (1.0)	929 (1.0)
Cell current, A	Assumed	50	50
Current density, mA/cm^2 (A/ft^2)	Calculated	53.8 (50)	53.8 (50)
Stoichiometric flow rate at 90 percent DOD cm^3/min	table V	312	312
Stoichiometric flow rate multiplier	Fig. 13	1.5 F_{SF}	1.5 F_{SF}
Flow rate per cell, cm^3/min	Calculated	468	1.5 F_{SF}
Stack size, number of cells	Assumed	40	40
Pump efficiency, percent	Assumed	60	60
Nominal stack power, w	Estimated	1800	1800
Flow-port dimensions, cm	Trials	0.81 by 0.23 by 20	0.43 by 0.08 by 20
Shunt loss (40-cell stack), w	Results from trial and error summing as a function of port sizes	37	11.2
Pump loss (40-cell stack), w		22	22.3
Minimum of shunt plus pump loss, w		59	33.5
Total losses during a complete charge/discharge cycle, WH (percent of discharge energy)	Shunt loss x 2 t_D* + pump loss x 2 x 2 t_D*	162 t_D (9.0)	112 t_D (6.2)

*t_D = discharge time = charge time.

TABLE VII. - SUMMARY OF PUMPING LOSS ESTIMATES FOR

10 TO 90 PERCENT DOD CYCLE

[1-molar solutions; pump efficiency, 60 percent; constant current discharge, 53.8 mA/cm^2 (50 A/ft^2); solution capacity, 100 A•hr]

	Variable flow		Constant flow[a]	
	1.5 F_{SF}	2.0 F_{SF}	1.5 F_{SF}	2.0 F_{SF}
Electrical energy output, W-hr	70.30	71.11	72.85	73.03
Calculated single-cell pumping energy during discharge, W-hr	.09	.17	.85	1.60
Net energy, W-hr	70.21	70.94	72.00	71.43
Pumping loss, percent:				
Cell and stack; discharge only	.13	.24	1.17	2.19
Cell and stack; charge and discharge	.26	.48	2.34	4.38
Cell, stack, and plumbing; charge and discharge	.52	.96	4.68	8.76

[a]Calculated at 90 percent DOD.

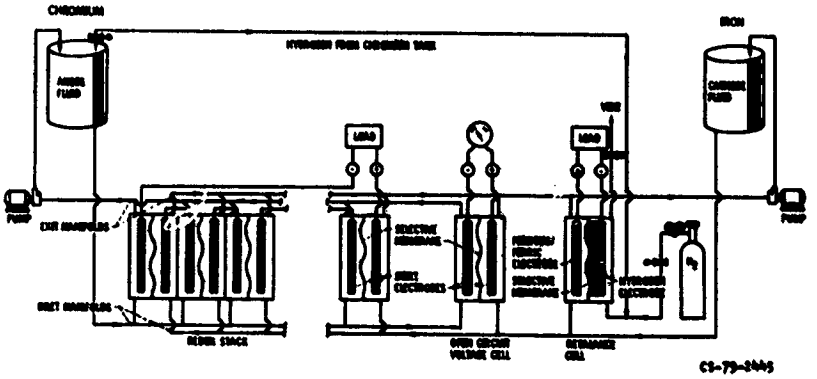

Figure 1. - Full function redox cell system.

ORIGINAL PAGE
BLACK AND WHITE PHOTOGRAPH

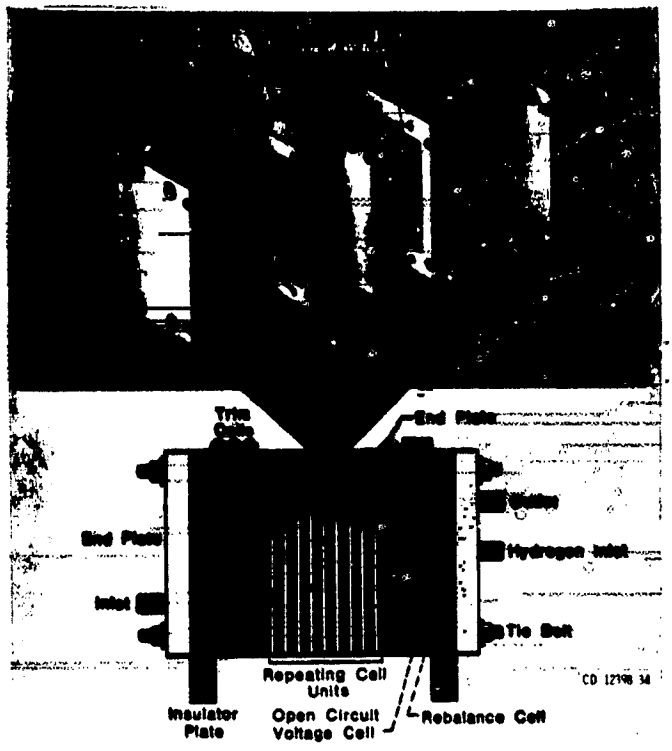

Figure 2. - Redox stack and single cell components.

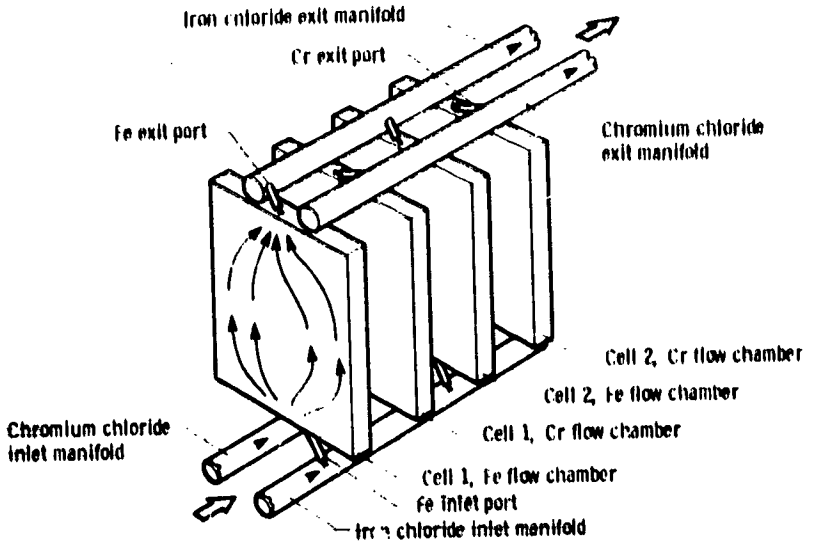

Figure 3. - Hydraulic network in a parallel-flow Redox stack.

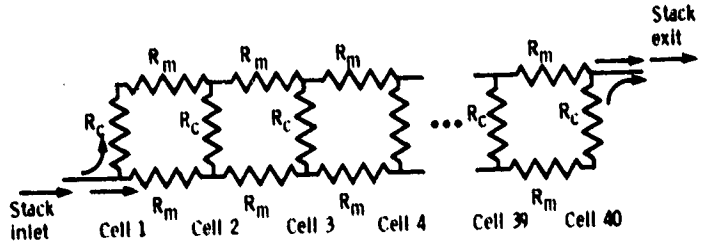

Figure 4. - Schematic representation of flow network of a multicell, parallel-flow cell stack. R_m is the resistance to flow along the segment of manifold from one cell to the next. R_c is the resistance to flow across a cell. This includes the inlet and outlet ports as well as the felt-filled cell cavity.

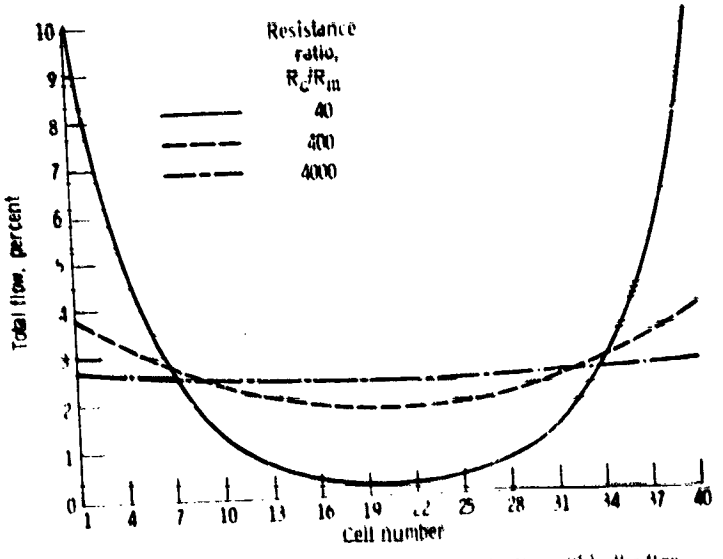

Figure 5. - Predicted cell-to-cell flow maldistribution within the flow network of figure 4.

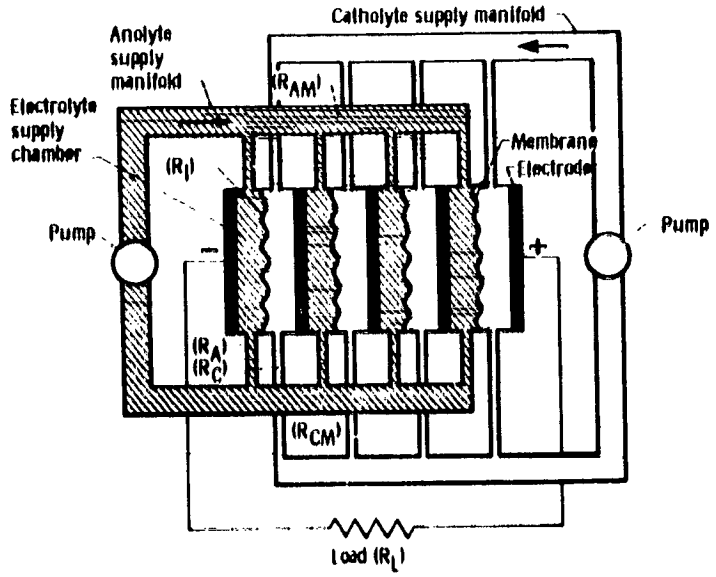

Figure 6. - Flow schematic of four-cell Redox system. Resistance in catholyte manifold, R_{CM}; resistance in catholyte port, R_C.

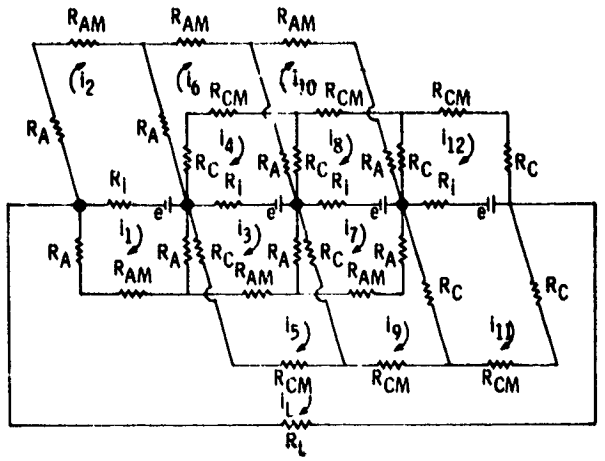

Figure 7. - Electrical analog of four-cell Redox system. Resistance in anolyte port, R_A; resistance in anolyte manifold, R_{AM}; internal resistance of cell, R_I; cell voltage (open circuit), e.

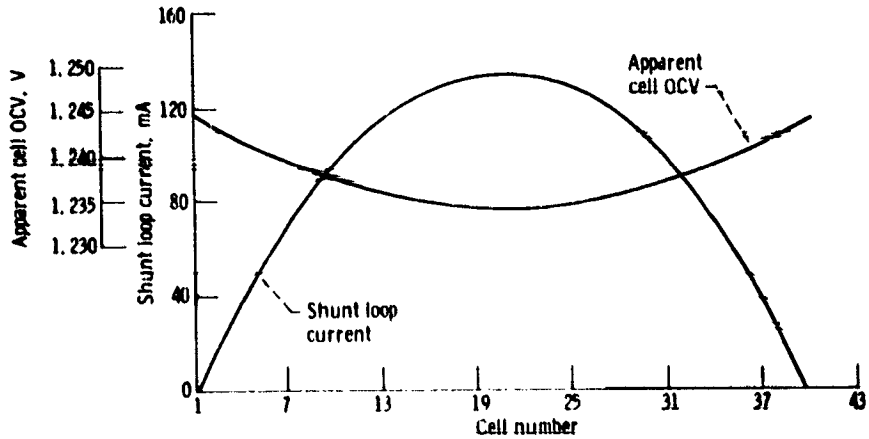

Figure 8. - Predicted shunt loop currents and resultant cell open-circuit voltages (OCV) in 40-cell stack. Cell ionic resistance, 1450 ohms; true OCV, 1.250 V.

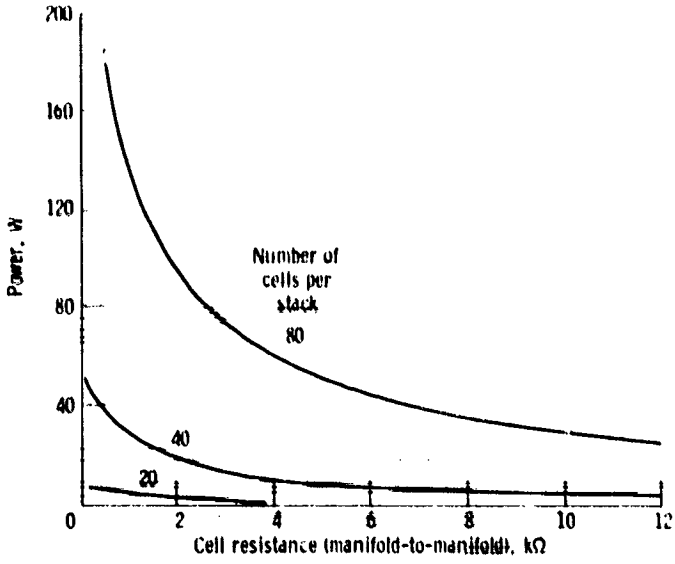

Figure 9. - Shunt losses per stack as predicted by NASA model. The magnitude of the shunt current losses increase with about the cube of the number of cells in the stack.

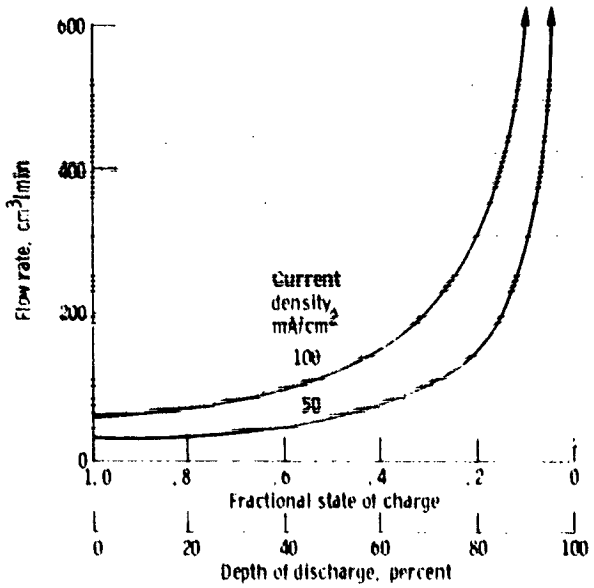

Figure 10. - Stoichiometric flow requirements of a 929-cm^2 cell during discharge for the case of 1.0 molar solutions.

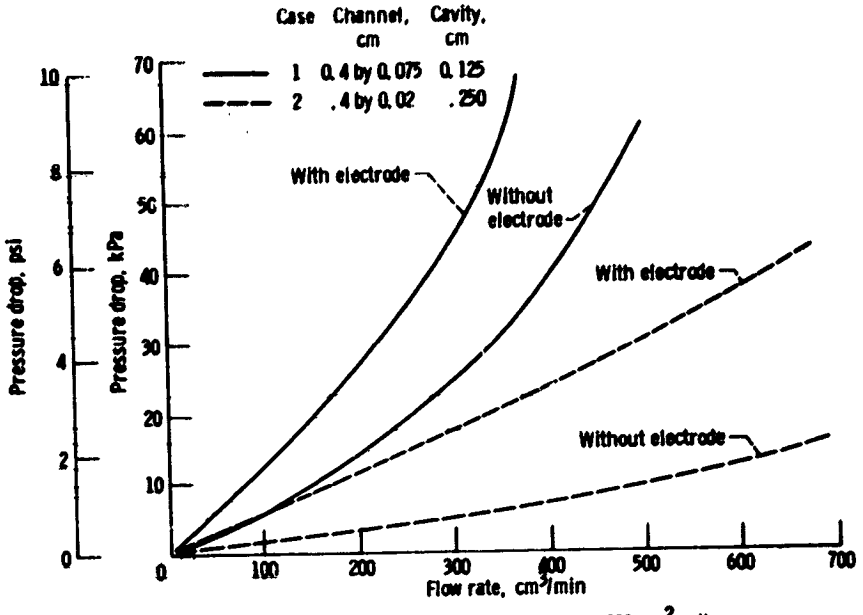

Figure 11. - Pressure drop versus flow rate for 929-cm^2 cell.

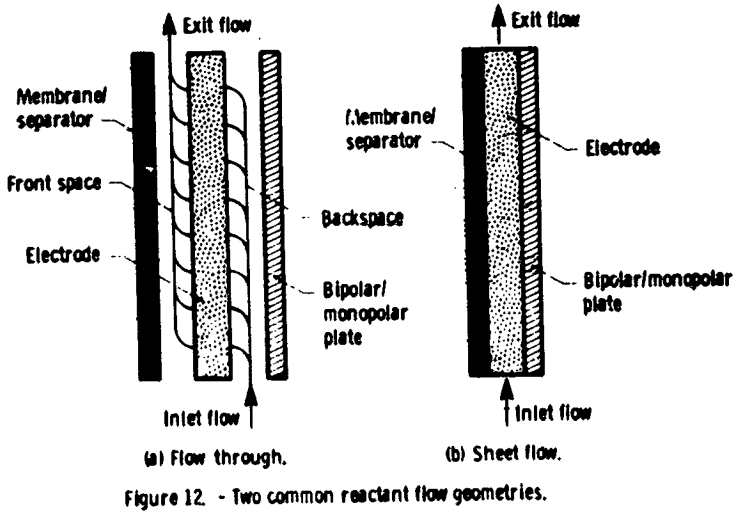

Figure 12. - Two common reactant flow geometries.

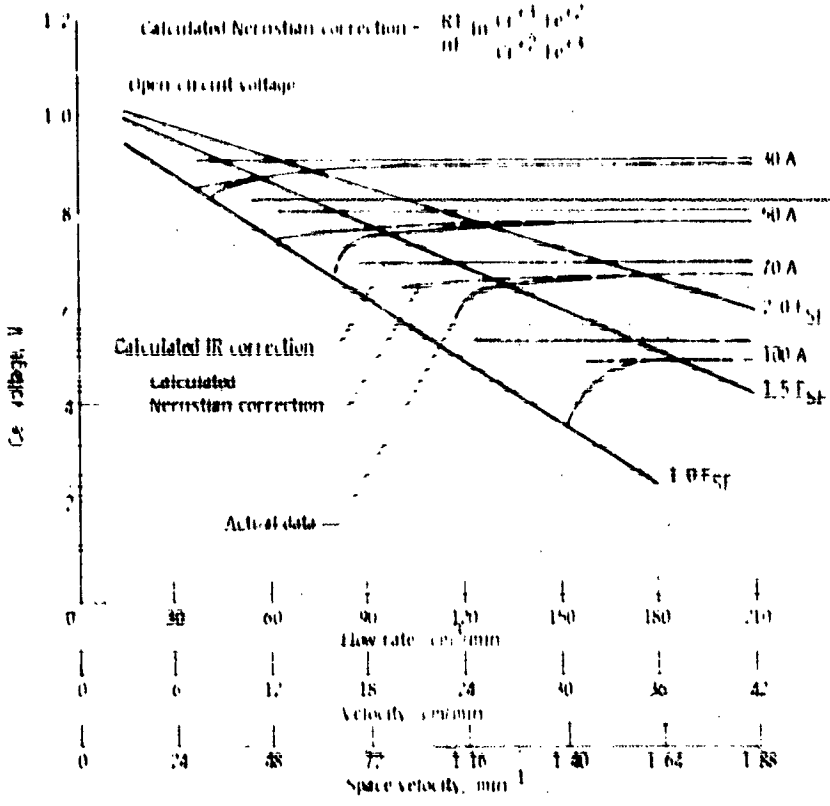

Figure 13. Performance map of 9.29 cm² simple cell. Depth of discharge, 50 percent.

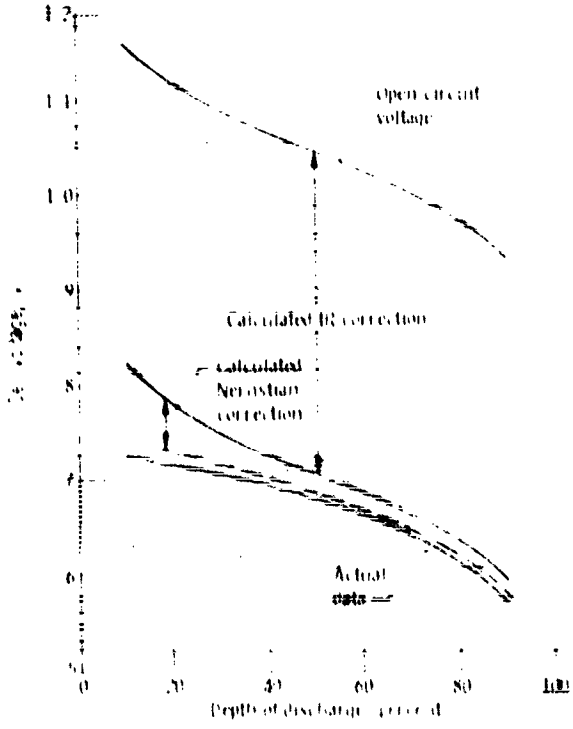

Figure 14. Evaluation of cell discharge performance. Current density, 54 A/cm²; flow rate, 70

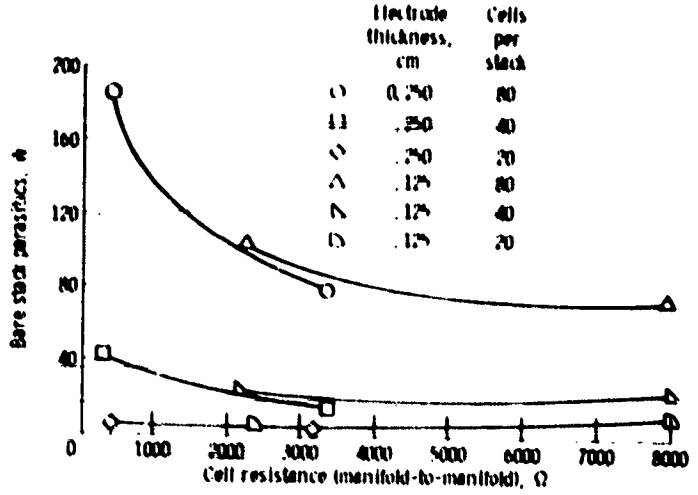

Figure 15. - Calculated sum of shunt power and pump power for flow cell stacks. Note: Calculations do not include stack-to-stack shunt losses or pumping losses outside of stacks. Flow rate, 150 cm^3/min per cell cavity; assumed pump efficiency, 60 percent; cell area, 929 cm^2.

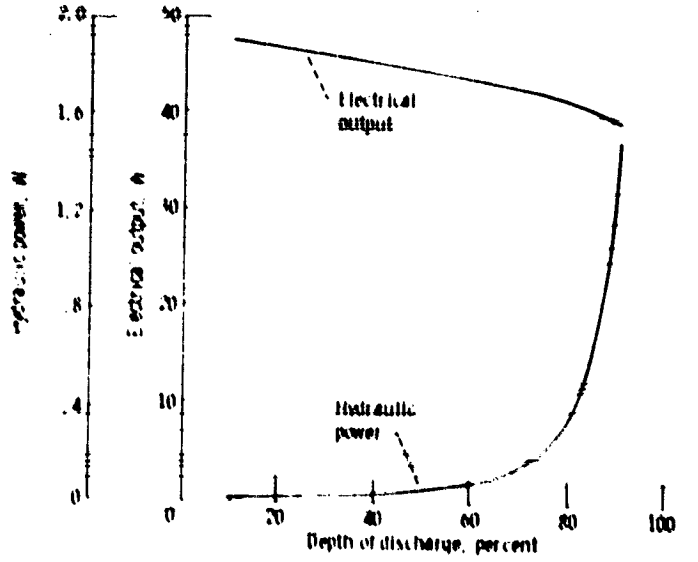

Figure 16. - Cell output and pumping requirements for experimental 929-cm^2 single cell. Constant current discharge, 50 A; solution capacity, 100 A hr; flow rate, 2.0 l/s; assumed pump efficiency, 40. Gross cell output, 71.1 W hr; hydraulic loss per cell (both fluids), 0.1 W hr; net cell output, 70.8 W hr; pumping loss, 0.4 percent.